Fracture 1977, Volume 2, ICF4, Waterloo, Canada, June 19 - 24, 1977

DUCTILE FRACTURE INITIATION AND PROPAGATION IN FERRITIC S.G. CAST IRON

G. Jolley* and S. R. Holdsworth**

INTRODUCTION

Since the discovery of S.G. cast iron the mechanisms of ductile and brittle failure in ferritic S.G. cast iron, in particular, have been the subject of many research papers and until quite recently the proposed failure mechanisms have been based on tensile and impact test data.

Gilbert [1] has shown that ductile, fibrous failure in a ferritic iron occurs by fibrous tearing of the ferrite matrix with numerous graphite nodules appearing in the fracture path. His later work [2] showed that ductile failure of a ferritic S.G. iron is associated with considerable elongation of the graphite nodule in the direction of tensile stress with voids appearing at the primary/secondary graphite interfaces in annealed irons which then propagate through the matrix in a fibrous manner.

The role of graphite nodules in the transition from fibrous to cleavage fracture is perhaps not quite so clear. Figure 1 constructed from the work of Pellini, Sandoz, and Bishop [3] compares the notched charpy characteristics of a typical ferritic S.G. cast iron with the matrix material, 2.25% silicon ferrite. The lowering of the upper shelf charpy values by the introduction of graphite nodules into the matrix is a result of the role of graphite nodules in facilitating fibrous fracture as previously explained. Pellini et al [3] felt that the lowering of the transition temperature was caused by the graphite nodules acting as brittle crack arresters and showed photographs of brittle microcracks in association with nodules to support this view. One drawback of this explanation is that if it were the case one might expect to see evidence of these brittle microcracks at or near fracture surfaces of ferritic S.G. iron samples at any temperature beneath the transition temperature of the matrix material. Such cracks, however, are only seen on specimens tested in the transition range of the base material.

The effect of graphite nodule number and spacing on the impact properties of ferritic S.G. cast iron has been investigated by various workers [4,5]. It has been shown that increasing the nodule number and decreasing the spacing results in a lowering of the impact transition temperature and a decrease in the ductile impact value. Mogford and Hull [4] produced a linear relationship between graphite nodule spacing and impact transition temperature and concluded that this was due to the graphite nodules acting as brittle crack arresters. The lowering of the ductile impact value can again be adequately explained by the effect of graphite nodules in facilitating fibrous fracture.

*Department of Aeronautical and Mechanical Engineering, University of Salford, England.
**Central Metallurgical Laboratories, G.E.C. Whetsone, Leicester, England.

Design of S.G. iron components subjected to increasing stresses has necessitated more quantitative information on the fracture toughness of this material and a number of authors have published results on the linear elastic [6,7,8] and general yielding [7,8,9] fracture characteristics of the material. This work while providing data relating critical flaw size with applied stress has also provided information which can be used to describe the mechanisms of fracture of ferritic S.G. iron in the presence of a crack-like defect, when the conditions of fracture initiation are changed. In the present paper fracture toughness results on ferritic S.G. cast irons of varying nodule number and volume fraction will be presented and their implications to the mechanisms of ductile fracture initiation and propagation, in the presence of a pre-existing crack, will be discussed.

EXPERIMENTAL

Six S.G. cast irons supplied by the British Cast Iron Research Association were used in this work. The irons were cast to allow a variation in graphite nodule number, by inoculation technique, and a variation in graphite nodule volume fraction by changes in carbon content to be obtained in the same cast section size (4.5 cm keel blocks). All the irons were ferritised by a double anneal heat treatment which involved soaking at 900°C for 16 hours prior to furnace cooling to 690°C and holding at this temperature for 48 hours before furnace cooling to room temperature. Microexamination of the irons indicated an almost fully ferritic matrix containing approximately 4% volume fraction of retained pearlite. Tables 1 and 2 give the chemical compositions and metallographic details of the irons while Figure 2 gives some indication in the variation in graphite nodule size and dispersion.

Using the same materials a previously published work [7] was concerned with crack opening displacement (C.O.D.), and Kic values of ferritic S.G. cast iron, and in particular the effect of graphite nodule size and dispersion on C.O.D. transition, C.O.D. at maximum load, δ_{max}, and Kic values in the material. The C.O.D. testing facility described in this earlier paper was used for the present work as was the method of measuring C.O.D. and they will not therefore be described in this paper. The specimens used in the present tests were fatigue pre-cracked 20 mm x 10 mm specimens 50 mm long with an a/w ratio of o.5; further details can be obtained from the previous paper [7].

In order to investigate the effect of graphite nodule size and dispersion on the initiation of ductile fracture, the effect of these variables on, δ_i, the C.O.D. at fibrous crack initiation, was studied. An examination of the fracture surfaces of the testpieces used to produce the C.O.D. temperature transition curves enabled plots of fibrous crack growth versus C.O.D. to be prepared. Figure 3 shows the six relationships for the irons examined. δ_i was the C.O.D. associated with no fibrous crack growth and was determined from the fibrous crack length C.O.D. relationships. Dixon [10] obtained δ_i isothermally for a ferritic S.G. iron at temperatures within the transition range and showed it to be independent of test temperature (Figure 4). His evidence confirms the validity of using the athermal method to determine δ_i for this material.

It can be seen from Figure 3 that δ_i is constant for all the irons examined and that the value of 0.05 mm is unaffected by changes in nodule size and volume fraction. There is unpublished collaborative evidence [9]

to suggest that this value of δ_i is yielded by irons exhibiting much higher and lower nodule numbers. In view of these initially rather surprising results it was decided to investigate the initiation sites of the fractured specimens using a scanning electron microscope. Fracture initiation in a fracture toughness specimen will start in the central region immediately beneath the fatigue crack; propagation then proceeding laterally and forwards through the specimen thickness in the plane of the crack. Figure 5 shows an area from this region in a broken specimen which shows evidence of intergranular fracture beneath the fatigue crack. This contrasts sharply with Figure 6 which is an area immediately beneath the fatigue crack away from the central region. Other work [9] has supported these findings and shown that ductile initiation areas can be intergranular or transgranular but do not seem to be associated with graphite nodules to the same extent as the rest of the fracture surface.

The role of the graphite nodules in the propagation of fibrous fracture in fatigue pre-cracked fracture toughness specimens is much the same as could be predicted from past work on impact tests. It can be seen from Figure 3 that, at any given value of C.O.D. in excess of δ_i, fibrous crack growth was more extensive in the irons with the lowest interparticle spacing. Figure 7 shows the effect of graphite interparticle spacing on the charpy ductile impact values determined in these irons from 10 mm x 10 mm x 55 mm notched specimens. Assuming the energy of fracture initiation to be constant as indicated in Figure 3 it can be seen from Figure 7 that the ductile fracture propagation energy is proportional to the interparticle spacing. Figure 8 shows the C.O.D. at maximum load, δ_{max}, plotted against interparticle spacing in these irons. The relationship between plastic instability can also be seen to be proportional to graphite spacing. The C.O.D. transition temperatures are also plotted in this figure. The C.O.D. transition temperature in this case was taken as the temperature beneath which no fibrous crack growth occurred and this again showed a linear relationship with interparticle spacing.

DISCUSSION

The results of this work show that in the presence of a defect such as a fatigue crack the graphite nodule number and spacing exert no influence on the strain required to initiate ductile failure from this defect. This would be very surprising if initiation were to occur at graphite nodule/matrix interfaces as it does in the absence of a defect. Smith and Knott [11] showed in a sulphur bearing steel, where fracture initiated at inclusion/matrix boundaries, that δ_i was related to a critical gauge length ℓ which is the interparticle spacing at right angles to the crack tip so long as the notch width was less than ℓ. If the S.G. irons tested in this paper had behaved in a similar manner some variation in δ_i would have been expected from the materials tested. The fact that none was found together with the evidence of Figure 6 and other workers strongly supports the view that initiation of ductile failure from the fatigue crack is associated with the matrix and not the graphite nodules. It is not considered too significant that intergranular initiation is sometimes seen - whether transgranular or intergranular the evidence strongly suggests that initiation occurs away from the graphite nodules which is the more significant point.

Once initiation has occurred graphite nodules facilitate the process of crack propagation as evidenced from Figures 3, 7 and 8. It is felt that this fact also explains the effect of variation in nodule size and dispersion on the transition temperature. Any factor which lowers the energy requirements for ductile crack propagation will lessen the risk of cleavage fracture. This explains the lower transition temperatures of the higher nodule number irons. Figure 9 taken from earlier work [7] shows that ductile crack growth occurs in this material down to very low temperatures; fully brittle cleavage fractures only occurring at the lower end of the transition range when the effect of graphite nodules as 'brittle crack stoppers' might become more important.

In the presence of a pre-existing sharp defect, therefore, it is suggested that ductile fracture in ferritic S.G. cast iron initiates in the matrix independent of graphite nodules which then play a part in ductile propagation; the finer the nodule size and dispersion the lower the energy for ductile crack growth and the less the likelihood of cleavage giving a lower fibrous/cleavage transition temperature. This latter point offers an acceptable alternative explanation of the phenomena shown in Figure 1. This mechanism also explains the rather low elongation figures noticed in samples taken from ferritic S.G. iron spun pipe containing surface defects from the casting operation. These irons have a very high nodule count and from the foregoing arguments would show a relatively low resistance to ductile fracture propagation in the presence of a pre-existing crack or defect. The very low transition temperature in this material resulting from the fine graphite dispersion is not necessarily advantageous since the service temperatures are well above this range.

Alternatively the use of large section size ferritic S.G. iron castings with a very large graphite nodule spacing might be expected to show greater fracture resistance so long as the service temperature is in the ductile range. However with larger section sizes the purity becomes more important since microsegregation of carbide forming elements can result in areas of retained massive carbide which can be harmful to the ductility of the material [5]. More work is in progress to investigate these possibilities which should be of interest to producers and users of large S.G. iron castings.

ACKNOWLEDGEMENTS

The authors are indebted to British Cast Iron Research Association, in particular Mr. G. N. J. Gilbert for provision of materials and helpful discussion.

REFERENCES

1. GILBERT, G. N. J., B.C.I.R.A. Jnl. 4, July 1953, 458.
2. GILBERT, G. N. J., B.C.I.R.A. Jnl. 12, July 1964, 170.
3. PELLINI, W. S., SANXOZ, G. and BISHOP, H. F.,Trans. A.S.M., 46, 1954, 418.
4. MOGFORD, I. L. and HULL, D.,Journal of the Iron and Steel Institute, January 1968, 79.
5. JOLLEY, G. and GILBERT, G. N. J.,British Foundryman, 60, March 1967, 79.
6. NANSTAD, R. K., WORZALA, S. J. and LOPER JNR, C. R.,Proc. 2nd Int. Symposium on "Metallurgy of Cast Iron" Geneva, May 1974, 589. Georgi Publishing Co.

7. HOLDSWORTH, S. R. and JOLLEY, G., Ibid, 810
8. HOLDSWORTH, S. R. and JOLLEY, G., British Foundryman, 68, June 1975, 169.
9. SCHOFIELD, R., HOPKINS, P. and JOLLEY, G., International Journal of Pressure Vessels and Piping, in press.
10. DIXON, G., Undergraduate project report, Dept. of Mechanical Engineering, University of Salford, July 1975.
11. SMITH, R. F. and KNOTT, J. F., Practical application of fracture mechanics to pressure vessel technology, Institute Mechanical Engineers 1971, C9/71, p 65.

Table 1 Chemical Composition of Irons Under Test

Iron	Chemical Composition							Inoculant
	C%	Si%	Mn%	S%	P%	Ni%	Mg%	
1	3.64	2.38	0.35	0.016	0.024	0.88	0.072	½%Fe/Si
2	3.62	2.41	0.34	0.016	0.024	0.83	0.064	½%Fe/Si + Bi
3	3.63	2.42	0.32	0.016	0.024	0.83	0.010	½%Fe/Si
4	2.58	2.16	0.45	0.020	0.025	0.81	0.054	½%Fe/Si
5	3.99	2.34	0.39	0.014	0.025	0.88	0.078	½%Fe/Si
6	3.23	2.28	0.41	0.016	0.024	0.84	0.065	½%Fe/Si
7	3.65	2.42	0.38	0.018	0.024	0.87	0.068	1%Fe/Si

Table 2 Metallographic Details of Irons 1-6

Iron No	Nodule N_L mm^{-1}	Number N_A mm^{-2}	Mean Interparticle Spacing mm	Mean Diameter mm	Volume Fraction Graphite %	Ferrite Grain Size ($\bar{L}$) mm
1	2.96	37.2	0.1390	0.0315	12.25	0.0214
2	3.89	106.8	0.0749	0.0277	12.12	0.0215
3	3.31	52.4	0.1133	0.0315	12.24	0.0221
4	1.87	20.6	0.1912	0.0366	8.58	0.0214
5	3.36	73.8	0.0942	0.0280	12.62	0.0205
6	2.65	40.0	0.1334	0.0314	10.86	0.0215

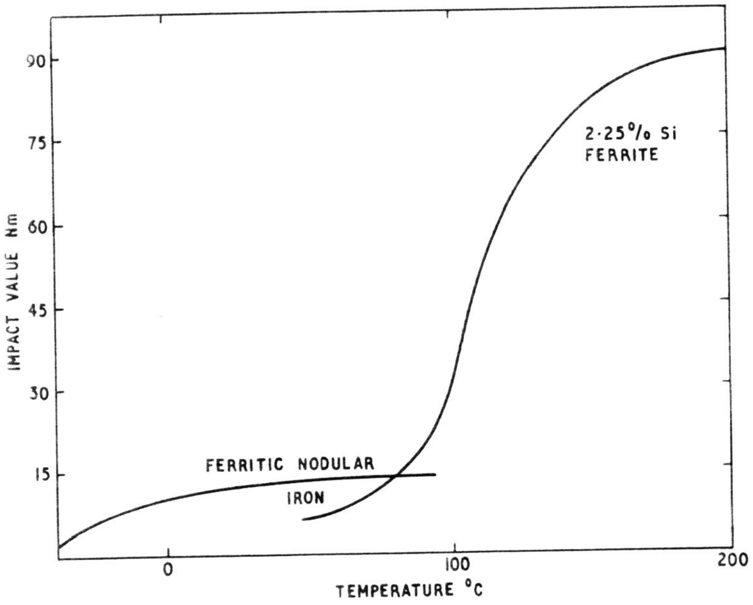

Figure 1 Comparison of the impact characteristics of ferritic S.G. iron and 2.25% δ_{i} ferrite, compiled from reference [3].

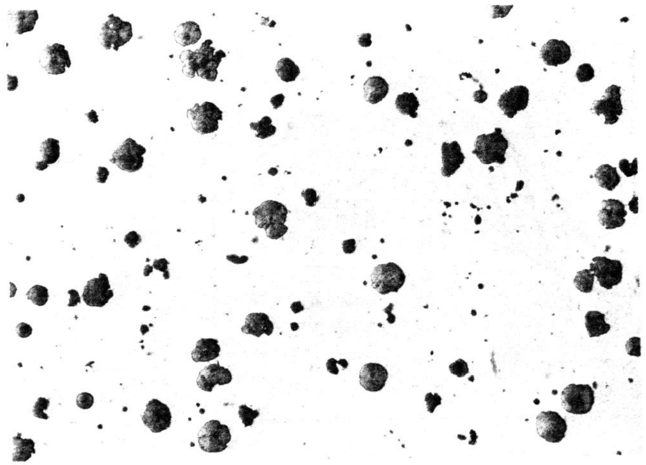

(a) iron 1

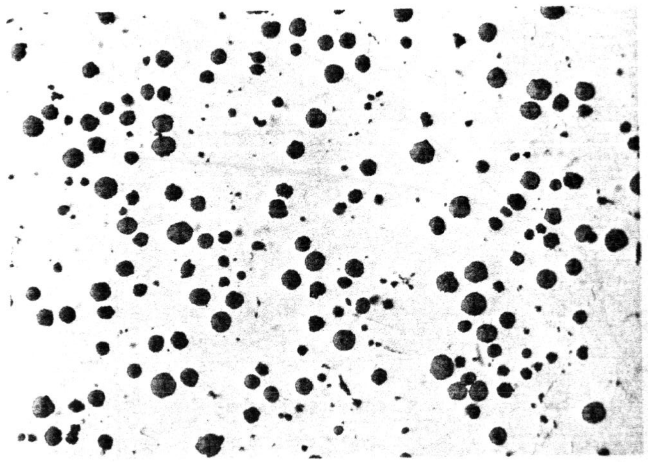

(b) iron 2 x 80 unetched

Figure 2 Examples of irons with a low and high internodule spacing

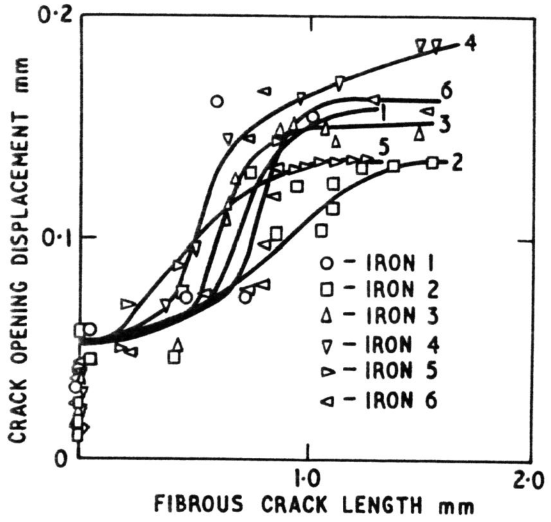

Figure 3 C.O.D./fibrous crack growth relationships for all the irons investigated

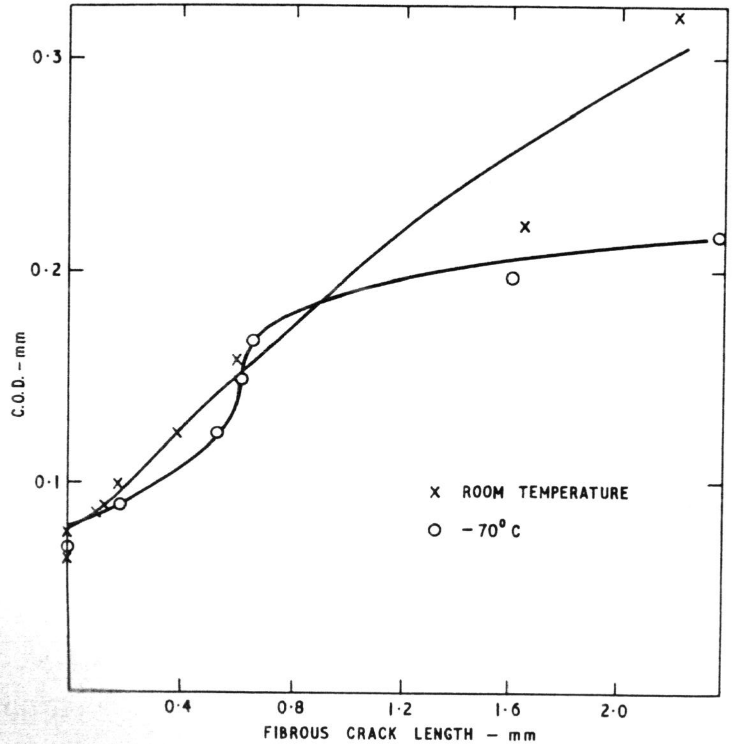

Figure 4 Effect of temperature on δ_i in a ferritic S.G. iron after Dixon [10]

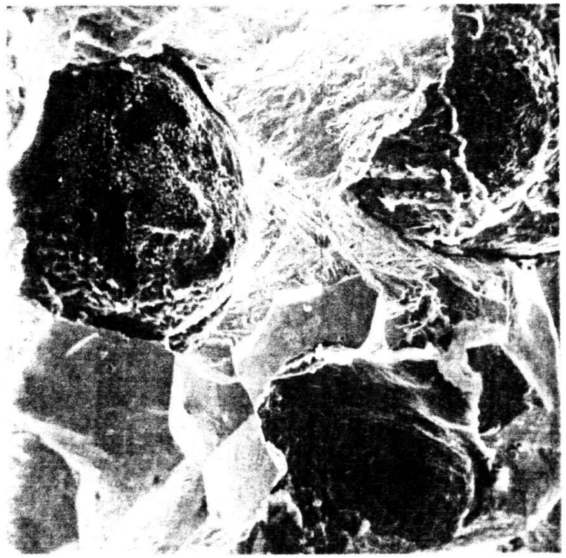

Figure 5 Intergranular initiation from tip of a fatigue crack (top of photograph) x 1000

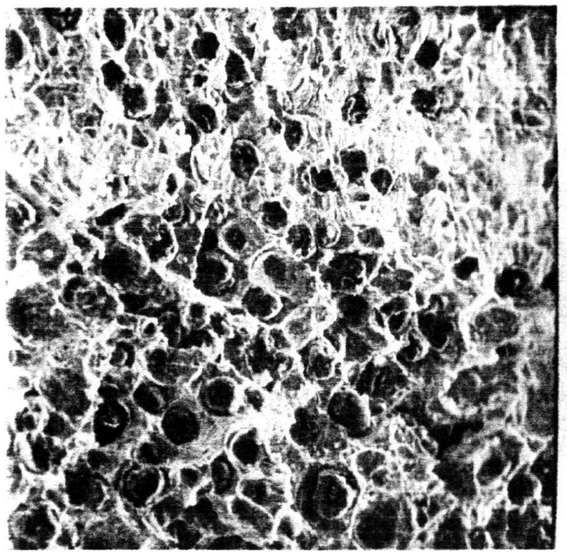

Figure 6 Normal fibrous fracture beneath fatigue crack (top of photograph) x 105

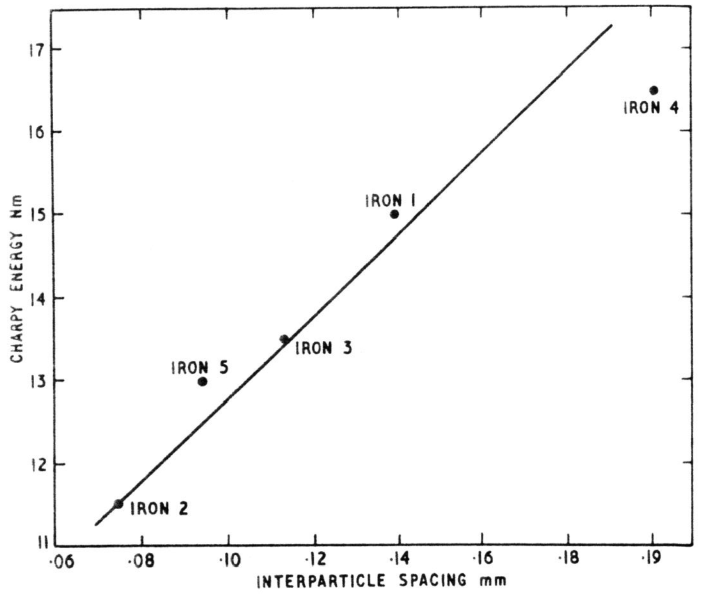

Figure 7   Effect of graphite interparticle spacing on charpy upper shelf values

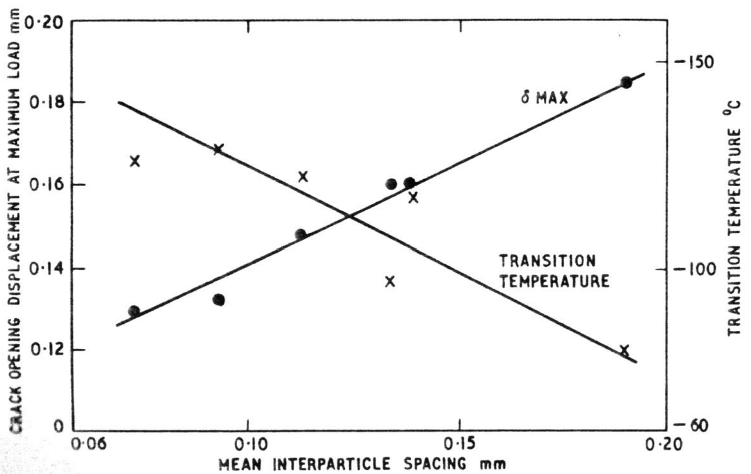

Figure 8   Effect of graphite interparticle spacing on δ_{max} and C.O.D. transition temperature

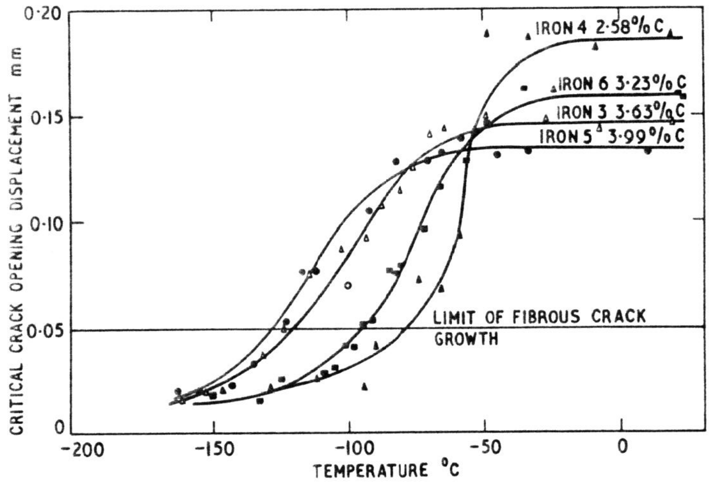

Figure 9   C.O.D. transition curves for 4 of the irons examined [7]